Article

Effect of Ni(NO$_3$)$_2$ Pretreatment on the Pyrolysis of Organsolv Lignin Derived from Corncob Residue

Wenli Wang, Yichen Liu, Yue Wang, Longfei Liu and Changwei Hu *

Key Laboratory of Green Chemistry and Technology, Ministry of Education, College of Chemistry, Sichuan University, 29 Wangjiang Road, Chengdu 610064, Sichuan, China; wangwenli30@163.com (W.W.); liuyc@stu.scu.edu.cn (Y.L.); Yue_Wang@stu.scu.edu.cn (Y.W.); liulongfeiscu@163.com (L.L.)
* Correspondence: changweihu@scu.edu.cn; Tel.: +86-28-8541-1105

Abstract: The thermal degradation of lignin for value-added fuels and chemicals is important for environment improvement and sustainable development. The impact of pretreatment and catalysis of Ni(NO$_3$)$_2$ on the pyrolysis behavior of organsolv lignin were studied in the present work. Samples were pyrolyzed at 500 °C with an upward fixed bed, and the characteristics of bio-oil were determined. After pretreatment by Ni(NO$_3$)$_2$, the yield of monophenols increased from 23.3 *wt.%* to 30.2 *wt.%* in "Ni-washed" and decreased slightly from 23.3 *wt.%* to 20.3 *wt.%* in "Ni-unwashed". Meanwhile, the selective formation of vinyl-monophenols was promoted in "Ni-unwashed", which indicated that the existence of nickel species promoted the dehydration of C$_\alpha$-OH and breakage of C$_\beta$-C$_\gamma$ in pyrolysis. In comparison with "Water", HHV of bio-oil derived from "Ni-unwashed" slightly increased from 27.94 mJ/kg to 28.46 mJ/kg, suggesting that the lowering of oxygen content in bio-oil is associated with improved quality. Furthermore, the content of H$_2$ in gas products dramatically increased from 2.0% to 7.6% and 17.1%, respectively.

Keywords: lignin; Ni(NO$_3$)$_2$·6H$_2$O; pyrolysis; pretreatment; bio-oil

1. Introduction

As environmental pollution and the depletion of fossil resources have become more serious, people have paid more attention to lignocellulosic biomass, which is an environmentally-friendly and renewable resource [1–3]. Lignin, cellulose, and hemicellulose are the three major components of lignocellulosic biomass. At present, the conversion of carbohydrates in biomass (cellulose and hemicellulose) to cellulosic ethanol and biogas has been well developed [1,4,5]. Lignin left by these utilizations of lignocellulosic biomass were considered as an undesired by-product. Except for some applications such as lignosulfonate [6], those lignin residues were burned to generate heat energy at a low utilization efficiency. Moreover, lignin had the highest H/C$_{eff}$ ratio among the three main components of biomass, implying that lignin had more potential in conversion into fuels with high energy density [7,8]. Therefore, the development of sustainable and efficient ways to convert lignin into chemicals or fuels is much needed.

The considerable research about the depolymerization of lignin has mostly focused on gasification, pyrolysis, hydrocracking, hydrolysis, and reduction or oxidative transformation [5,9]. Among these methods, pyrolysis was considered as one of the most feasible methods to convert all the components of biomass directly into value-added chemicals or fuels. This is similar to one-pot methods [9,10], where biomass was heated up to high temperature within the range of 450–650 °C in an inert atmosphere, obtaining gas, solid and liquid (namely bio-oil) products. The direct pyrolysis of lignin yielded less bio-oil and the liquid products contained less valuable phenolic monomers, but more undesirable oligomers and water. Wang et al. [11] obtained 25% of liquid using lignin derived from agricultural crop residues via direct pyrolysis. To improve the quality and yield of bio-oil, pretreatment of lignin and catalytic pyrolysis could be promising methods [5,12].

In the last decades, various pretreatment methods have been explored by researchers, such as dilute acid hydrolysis [12,13], alkaline pretreatment [12,14], autohydrolysis [15], steam explosion [12], ionic liquids pretreatment [16,17], and inorganic salt solution pretreatment [10,18]. Among these methods, pretreatment with inorganic salt solution is an outstanding and feasible means due to high efficiency and low cost [10,19]. Wang et al. [20] proposed a new conversion method called salt soaking−torrefaction. It was discovered that the pretreatment of $AlCl_3$ could stimulate the depolymerization of pubescens when torrefied at 200 °C, obtaining more bio-oil and phenolic monomers. Zhou et al. [21] pretreated technical lignin with $Ca(OH)_2$ easily, and approximately 38 *wt*.% yield of bio-oil was obtained at 450 to 600 °C, while agglomeration was efficiently improved.

Furthermore, catalytic pyrolysis of lignin was investigated because of the disadvantage of bio-oil derived from direct pyrolysis, which included high oxygen content, high viscosity, and instability [5,22]. Different catalysts, for instance zeolites [23], alkaline additive [24], metal oxide [25], metal chlorides [26], and mesoporous materials [27] were investigated to convert biomass or lignin into high-value products. Wang et al. [11] prepared AAEMs-loaded char as an ex-situ catalyst to study the interaction of volatile and char while lignin was catalytically pyrolyzed. They found that the yields of phenol, o-cresol, p-cresol and catechol in bio-oil increased, which was the results of demethylation, demethoxylation, or alkyl substitution. Jelena et al. [22] prepared three types of catalysts contained NiO marked as NiO/H-ZSM-5, NiO/H-β and NiO/H-Y, and investigated the catalytic pyrolysis of Eucalyptus and mixture of birch and aspen. They found that these catalysts all enhanced $Y_{aromatics}$ and decreased $Y_{oxygenates}$ in contrast with the control group. Therefore, it is meaningful to increase the yield and figure out the reaction pathway in order to make lignin more useful.

In this study, organosolv lignin obtained from corncob residues was selected as the feedstock due to little modification with lignin structure. The investigation of lignin pyrolysis could provide useful information for pyrolytic conversion of biomass to upgrade the quality of bio-oil. To explore the thermal degradation of lignin at 500 °C and obtain higher yield and better quality of bio-oil via lignin pyrolysis, the pretreatment of nickel nitrate on organsolv lignin was studied. The results revealed that $Ni(NO_3)_2$ pretreatment efficiently influenced the pyrolysis performance of organsolv lignin, showing differences in char, gas, and bio-oil products.

2. Materials and Methods

2.1. Feedstocks

Corncob residue was collected from Shandong Futaste Investment Co., Ltd. (Qingdao, Shandong Province, China). Corncob residue was an industrial waste left from the catalytic hydrolysis of hemicellulose to produce xylose, which meant cellulose and lignin were the major components of corncob residue [28]. The details of extraction of organsolv lignin (OL) from corncob residue and related characterizations can be found in our previous study [29]. All chemicals were used as received.

2.2. Pretreatment of OL with $Ni(NO_3)_2$

An aqueous solution of 10 *wt*.% $Ni(NO_3)_2$ was prepared using $Ni(NO_3)_2 \cdot 6H_2O$ of analytical grade. A quantity of 6 g of OL were immersed into the as prepared solution (30 g), and then stirred for 24 h at 17 °C. After soaking, the filtered mixtures were washed with 100 mL of pure water five times. Then the solid residues were freeze-dried at −105 °C and 80 mT before pyrolysis. Meanwhile, two control groups were prepared where OL was pretreated by 30 g of pure water and 10 *wt*.% $Ni(NO_3)_2$ aqueous solution but unwashed after filtration, respectively. OL pretreated by pure water, $Ni(NO_3)_2$ aqueous solution but washed or unwashed, were named "Water", "Ni-washed" and "Ni-unwashed", respectively.

2.3. Pyrolysis Experiment

In this experiment, upward fixed bed reactor was used and the schematic diagram could be found in our previous work [29]. The system contained three parts, which were reacting zone, cooling zone, and gas collection zone. The reacting zone consisted of two tubes (one inner and one outer) which were made of quartz, and cooling zone was made up by a spiral condenser submerged in ice water. A gas bag was used to collect the effluent, where N_2 acted as carrier gas. Before pyrolysis, the pyrolytic unit was purged with nitrogen for 15 min to get an inert atmosphere, and the rates of gas of inner and outer tubes were 40 and 60 mL/min, respectively. About 2.0 g of pretreated OL were put into the inner tube, and then heated up to 500 °C at 10 °C/min and then remained there for 2 h. The inner tube, outer tube, and spiral condenser were weighted before and after pyrolysis in order to calculate the yields of gas, char, and bio-oil. THF was used to wash spiral condenser to make up 25 mL solution for quantification and preservation.

The pyrolytic product yields were acquired with Equations (1)–(5) as follows:

$$m_{liquid} = (m_{ot} + m_{cond})_{after} - (m_{ot} + m_{cond})_{before} \tag{1}$$

$$m_{solid} = (m_{it})_{after} - (m_{it})_{before} \tag{2}$$

$$Y_{oil} = \frac{m_{liquid} - m_{6H_2O}}{m_{sample} - m_{Ni(NO_3)_2 \bullet 6H_2O}} \times 100\% \tag{3}$$

$$Y_{char} = \frac{m_{solid} - m_{6H_2O}}{m_{sample} - m_{Ni(NO_3)_2 \bullet 6H_2O}} \times 100\% \tag{4}$$

$$Y_{gas} = 100\% - Y_{char} - Y_{oil} \tag{5}$$

where m_{ot} and m_{it} represented the weight of outer and inner tube, respectively. m_{cond} represented the weight of cooling unit. The yield of gas was obtained by mass balance.

2.4. Methods of Analysis and Characterization

2.4.1. Characterization of Pretreated OL

Inductively coupled plasma-emission spectroscopy (ICP-AES) was used to determine the content of $Ni(NO_3)_2 \cdot 6H_2O$ in each sample. All samples were tested by an IRIS Advantage (TJA Solutions, New York, NY, USA) twice and take the average. 0.2 g pretreated OL were weighed in the beaker and 20 mL of HNO_3 was added to digest lignin. Then the solutions were heated to assist digestion of lignin until remained solution was about 3 mL, and were made up to 10 mL. Before the test, the solutions were diluted 20 times in case the acidity was too strong.

The Fourier Transform Infrared Spectra (FT-IR) was recorded on a Nicolet Nexus 670 Fourier transform infrared spectrometer in the range of 4000–400 cm^{-1} at a resolution of 2 cm^{-1} to observe variations of functional groups of lignin after soaking. Before the test, a small amount of pretreated OL were mixed with KBr, and then pressed into a transparent sheet.

X-ray diffraction (XRD) was used to observe the changes of the sample after soaking. The results were obtained from a PANalytical B.V. of EMPYREAN instrument at 2θ from 5 to 80° on Cu Kα radiation with 35 kV and 30 mA and then compared with standard cards.

2.4.2. Characterization of the Liquid Products

GC-MS (Agilent 6890N, Santa Clara, CA, USA) equipped with a polar INNOWax (30 m × 0.25 mm × 0.25 μm, HP) column was used to determine qualitatively small-molecular phenolic compounds in bio-oil. The temperature of inlet and mass detector were both 280 °C. Two minutes of solvent delay was displayed, and the oven, heated by a temperature programmed method, was set to increase from 50 to 200 °C at 3 °C/min.

The yields of identified small-molecular monophenols were determined with GC-FID (PerkinElmer Clarus GC, Waltham, MA, USA) which was equipped the same column with

GC-MS. The internal standard method (benzyl alcohol) was chosen to determine the yields of component in bio-oil. The temperatures of injector and detector maintained were 280 and 330 °C respectively. The oven, heated by a temperature programmed method, was set to increase from 50 to 200 °C at 3 °C/min, and then remained at this temperature for 2 min.

GPC (ACQUITY, Waters, Beverly, MA, USA) was used to analyze the molecular weight distribution of bio-oil, which was equipped with two columns (ACQUITY APC XT 125, 2.5 μm, and ACQUITY APC XT 45, 1.7 μm, 150 × 4.6 mm, Waters) and a RID (2414, Waters) [10]. Tetrahydrofuran (HPLC grade) was selected as the mobile phase at 0.5 mL/min. Columns and detector were maintained at 40 °C. Before the test, solvent was removed from bio-oil and then a HPLC grade of tetrahydrofuran was added to dissolve sticky bio-oil. Analysis of data were accomplished by Empower.

ESI−MS (LCMS−IT−TOF, Shimadzu, Kyoto, Japan) was used to examine the phenolic oligomers in bio-oil. Nitrogen was used as nebulizer gas and was set at a rate of 1.5 L/min, while the rate of mobile phase was set at 0.25 mL/min. Meanwhile, the detector voltage of instrument was 1.60 kV. The collision-induced dissociation (CID) energy for MS/MS was 25% [20]. Before the test, a small amount of bio-oil was obtained with a capillary pipet and then diluted by methanol to about 2 mL.

Two-Dimensional Heteronuclear Single Quantum Coherence Nuclear Magnetic Resonance (2D HSQC NMR) Spectra of bio-oil was performed with a Bruker ADVANCE 600 MHz spectrometer. The spectra were recorded at the range of 10–0 ppm and 220–5 ppm in ^{1}H- and ^{13}C-dimensions, respectively. The characteristic peak of deuterated dimethyl sulfoxide (δC/δH = 39.5/2.5 ppm) was used for chemical shift calibration. Before the test, the solvent was also removed and 0.55 mL of d_6-DMSO was used to dissolve bio-oil.

2.4.3. Characterization of the Gaseous Products

GC-TCD was used to determine the relative contents of gaseous products. The samples were tested by GC9710 (Fuli, Taizhou, China) equipped with a TCD detector and a TDX-1 carbon molecular sieve packed column (2 m × 3 mm id) [20]. The temperatures of column, detector and oven were maintained at 120, 145 and 160 °C, respectively. The flow rate of carrier gas (N_2) was 20 mL/min.

3. Results and Discussion

3.1. The Characteristics of Pretreated OL

The contents of nickel nitrate in pretreated OL were calculated according to Equation (6) and the results were listed in Table 1. As shown in Table 1, a small amount of nickel remained in "Ni-washed", which suggested that Ni^{2+} might be bonded to phenolic hydroxyl, aliphatic hydroxyl or carbonyl units to form complexes [30], which was difficult to be removed by water washing. In "Ni-unwashed", about 4.00 *wt.%* of nickel was left in the sample.

$$W_{Ni(NO_3)_2 \cdot H_2O} = \frac{m_{Ni(NO_3)_2 \cdot H_2O}}{m_{Ni(NO_3)_2 \cdot H_2O} + m_{lignin}} \qquad (6)$$

Table 1. The content of nickel nitrate in pretreated organsolv lignin (OL).

| Content/(*wt.%*)	Water	Ni-Washed	Ni-Unwashed
Ni	0.00 ± 0.00	0.03 ± 0.01	4.00 ± 0.71
$Ni(NO_3)_2 \cdot 6H_2O$	0.00 ± 0.00	0.10 ± 0.01	19.82 ± 0.71

The FT-IR spectra of pretreated OL were represented in Figure 1. According to the literature [24,29,31–33], the characteristic peaks were all assigned. The absorption at 1688 cm^{-1} and 1654 cm^{-1} were corresponding to conjugated C=O at α-position without C_β=C_γ and with C_β=C_γ, respectively. The peaks at 2931 and 2847 cm^{-1} were due to the stretching vibration of C-H in -OCH$_3$ groups. The peaks at 1630, 1601, 1512, 1452, and 1421 cm^{-1} represented the vibration of aromatic rings in lignin, while characteristic peaks

at 831 and 518 cm^{-1} were assigned to the deformation vibration of C-H bonds in aromatic rings. The bands at 1328 and 1122 cm^{-1} were due to stretching vibration and deformation vibration of syringyl unit (S), respectively. The bands at 1261 and 1165 cm^{-1} corresponded to guaiacyl rings (G). These peaks did not show apparent change. A broad absorption band at 3337 cm^{-1} was detected and it was attributed to phenolic or aliphatic O-H. Compared with the "Water", the peak intensity at 3337 cm^{-1} in "Ni-washed" was slightly lower, which might be also attributed to the effect of pretreatment with Ni(NO$_3$)$_2$. However, the intensity of the peak at the same wavenumber in "Ni-unwashed" increased due to the existence of Ni(NO$_3$)$_2$·6H$_2$O. The peak at 1028 cm^{-1} corresponded to the deformation vibration of aliphatic ether; the intensities of which in "Ni-washed" and "Ni-unwashed" were both slightly decreased.
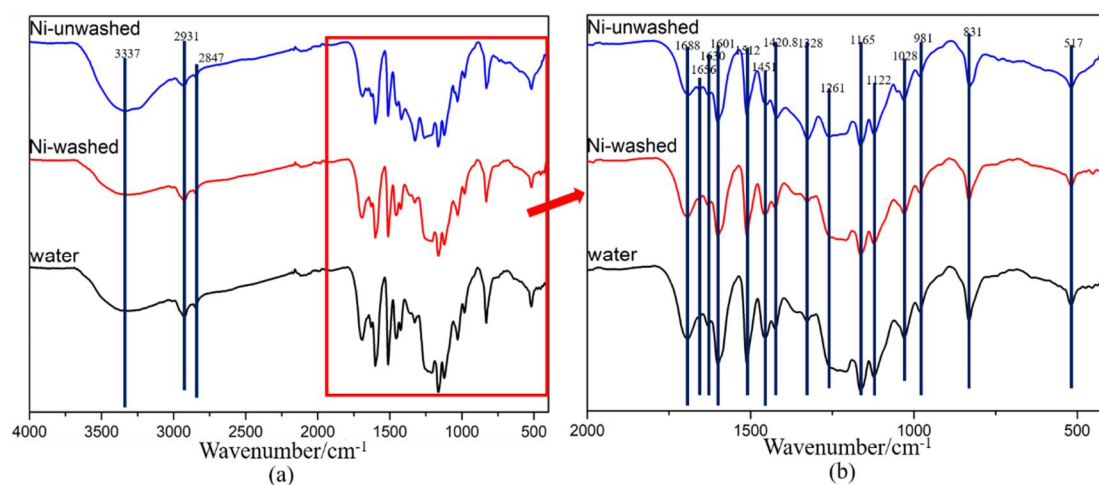
Figure 1. The FT-IR spectra of pretreated organsolv lignin in different ranges: (**a**) in the range of 4000–400 cm^{-1}; (**b**) in the range of 2000–400 cm^{-1}.

XRD was used to examine the possible variation of samples after pretreatment, and the XRD spectra of pretreated OL were shown in Figure 2. Compared with standard cards (PDF01-0204), the peaks at 16.102°, 21.44°, 23.516°, 26.188° and 32.655° showed the existence of Ni(NO$_3$)$_2$·6H$_2$O in "Ni-unwashed". However, Ni(NO$_3$)$_2$·6H$_2$O was not detected in "Ni-washed". Therefore, it was reasonable to deduct the content of Ni(NO$_3$)$_2$·6H$_2$O when calculating the yields in pyrolysis reaction. Meanwhile, the broad peak ranging from 19 to 25° could be assigned to the amorphous carbon (002) [34,35].
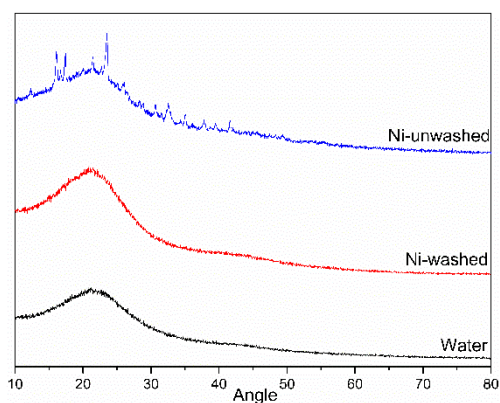
Figure 2. The X-ray diffraction (XRD) spectra of pretreated organsolv lignin.

3.2. Pyrolysis Products Distribution

The pyrolytic product yields at 500 °C were listed in Table 2, and the yields were obtained based on Equations (1)–(5). When OL was pretreated with water, the yields of char,

bio-oil and gas were 45.44 *wt.%*, 36.50 *wt.%* and 18.15 *wt.%*, respectively. Francois-Xavier Collard et al. [36] used commercial lignin (alkali, Aldrich 370959, St. Louis, MO, USA) as raw material to study its pyrolysis behaviors at 600 °C, and the corresponding yields of char and gas in their work were 45.4 ± 1.0%, and 14.0 ± 0.9%, respectively. The differences in yields might result from the difference of feedstock and pyrolysis temperature.

Table 2. Yields of char, bio-oil, and gas products after pyrolysis at 500 °C (*wt.%*).

Lignin Samples	Conversion	Char	Bio-Oil	Gas
Water	54.60 ± 0.42	45.44 ± 0.48	36.50 ± 0.14	18.15 ± 0.35
Ni-washed	55.05 ± 0.78	44.95 ± 0.78	35.55 ± 0.346.5	19.50 ± 0.62
Ni-unwashed	52.34 ± 0.64	47.66 ± 0.96	32.81 ± 0.78	19.52 ± 0.26

Compared with "Water", the yields of char, bio-oil and gas in "Ni-washed" showed a small difference in yields of gas and bio-oil while the conversion did not change, which revealed that the pretreatment of Ni(NO$_3$)$_2$ had little impact on the yield distribution of the products in the three phase. Part of the difference in the char fraction might be due to the existence of nickel in char derived from Ni(NO$_3$)$_2$ in the "Ni-washed". In "Ni-unwashed", the yields of char and gas slightly increased from 45.44 to 47.66 *wt.%* and from 18.15 to 19.52 *wt.%*, respectively, while the yield of bio-oil decreased from 36.50 to 32.81 *wt.%*. It was implied that the depolymerization of lignin was inhibited, leading to decrease in bio-oil. Furthermore, it could be the effect of nickel in "Ni-unwashed" that promoted the cleavage of the side chain in lignin structure, yielding more gas products in pyrolysis. According to Francois- Xavier Collard et al. [36], pyrolysis of commercial lignin pretreated by nickel nitrate yielded 49.4 ± 0.4% of char and 14.7 ± 0.1% of gas. Similar results were reported by Bru et al. [30], where aqueous solution of Ni or Fe nitrates was used to immerse oak wood, and the yields of char and gas products increased at a sacrifice of liquid product by pyrolysis at 700 °C. Nickel/iron nitrate were used to impregnate cellulose by Francois-Xavier Collard et al. [37] and they discovered a decrease of tar through fast pyrolysis. The results in the present work were generally consistent with those literature results.

3.3. The Characteristics of Bio-Oil

The elemental composition of the bio-oil obtained from pyrolysis was determined by Elemental analysis. As listed in Table 3, the bio-oil mainly contained C, N, O and H, whereas S was not detected. The corresponding HHV of bio-oil was obtained by Dulong formula. The pretreatment of Ni(NO$_3$)$_2$ has no significant effect on the element composition and HHV of the bio-oil. In comparison with "Water", the content of oxygen in bio-oil slightly decreased from 25.65 to 24.11 *wt.%* and HHV of bio-oil increased from 27.94 mJ/kg to 28.46 mJ/kg in "Ni-unwashed". It was speculated that the presence of nickel in sample had a positive influence on the removal of oxygen from bio-oil and improve the quality of pyrolytic bio-oil.

Table 3. Element Analysis of bio-oil derived from pyrolysis.

	C/*wt.%*	H/*wt.%*	O [a]/*wt.%*	N/*wt.%*	HHV (mJ/kg) [b]
Water	66.38 ± 1.42	7.07 ± 0.12	25.65 ± 1.55	0.90 ± 0.01	27.94 ± 0.93
Ni-washed	66.81 ± 0.16	6.98 ± 0.01	25.38 ± 0.17	0.83 ± 0.01	27.87 ± 0.11
Ni-unwashed	67.48 ± 0.89	7.02 ± 0.08	24.11 ± 0.98	1.39 ± 0.01	28.46 ± 0.58

[a] The content of O was calculated by mass balance; [b] Dulong formula: HHV(KJ/Kg) = 337 × C + 1419 × [H − 1/8 × O] + 93 × S + 23.26 × N.

3.3.1. Monophenols in Bio-Oil

Small-molecule monophenols were analyzed by GC−MS. The software of GC-MS made a possible speculation of these compounds, as shown in Figure 3. However, we could

not identify compounds of 17–20 precisely due to the lack of standard chemicals so we ignored to discuss those compounds in GC-FID results. Based on Equation (7), the yield of each compound was obtained and shown in Table 4.

$$Y_{comp} = \frac{m_{comp}}{m_{liquid} - m_{Ni-6H_2O}} \times 100\% \tag{7}$$
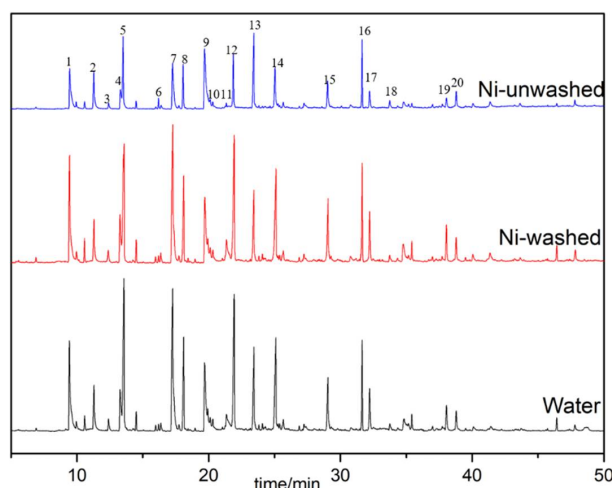
Figure 3. The GC-MS spectra of bio-oil derived from pyrolysis (1: phenol; 2: Benzyl alcohol; 3: o-cresol; 4: p-cresol; 5: guaiacol; 6: 2-ethylphenol; 7: 4-ethylphenol; 8: 4-methylguaiacol; 9: 4-vinylphenol; 10: 4-isopropylphenol; 11: 3-methoxycatechol; 12: 4-ethylguaiacol; 13: 4-vinylguaiacol; 14: syringol; 15: 4-methylsyringol; 16: butylated hydroxytoluene); 17: 5-tert-butypyrogallol; 18: 3-tert-butyl-4-hydroxyarisole; 19: ethyl 2-(4-hydroxy-3-methoxyphenyl)acetate; 20: 2,6-dimethoxy-4-(2-propenyl-)phenol.

Table 4. Yields of Small-Molecule compounds (on the basis of the weight of bio-oil) (*wt.%*).

	Compound	Water	Ni-Washed	Ni-Unwashed
	phenol	3.2	4.4	2.8
	o-cresol	0.3	0.3	0.2
	p-cresol	1.2	1.5	1.1
	2-ethylphenol	0.0	0.1	0.1
H	4-ethylphenol	3.4	4.5	1.9
	4-vinylphenol	2.7	3.0	4.4
	4-isopropylphenol	0.1	0.2	0.1
	3-methoxycatechol	1.0	1.6	0.8
	$\sum$H	11.9	15.6	11.4
	Guaiacol	3.1	4.1	2.0
	4-methylguaiacol	1.5	1.9	1.1
G	4-ethylguaiacol	2.1	2.7	1.0
	4-vinylguaiacol	1.3	1.5	2.1
	$\sum$G	8.0	10.2	6.2
	Syringol	2.2	3.0	1.6
S	4-methylsyringol	1.2	1.6	1.1
	$\sum$S	3.4	4.6	2.7
	Total (*wt%*)	23.3	30.2	20.3

The results in Table 4 were the average of two tests.

All small-molecular compounds identified could be classified into three groups based on the primary units of lignin: syringyl (S), guaiacyl (G), and p-hydroxyphenyl units (H). Phenol, o-cresol, p-cresol, 2-ethylphenol, 4-ethylphenol, 4-vinylphenol, 4-isopropylphenol, and 3-methoxycatechol were attributed to H type whose structure did not consist of -OCH$_3$.

Guaiacol, 4-methylguaiacol, 4-ethylguaiacol, and 4-vinylguaiacol were attributed to G type with one -OCH_3 at C_2 position. Syringol and 4-methylsyringol were attributed to S type with two -OCH_3 at C_2 and C_6 position. These compounds could be obtained through different mechanism of chemical bond cleavage in pyrolysis. According to literature [20,29,38], phenol, guaiacol, and syringol were acquired by the cleavage of C_1-C_α from primary units in lignin structure, while monophenols with methyl at C_4 position were mainly derived from the breakage of C_α-C_β in the side chain. Meanwhile, monophenols with ethyl at C_4 position were obtained from the breakage of C_β-C_γ while monophenols with vinyl at C_4 position could be attributed to the cracking of C_β-C_γ and the dehydration of C_α-OH.

In comparison to "Water", as shown in Table 4, the contents of determined monophenols increased except for o-cresol in "Ni-washed". It was inferred that the pretreatment of $Ni(NO_3)_2$ influenced the natural structure of lignin and promoted the formation of monophenol intermediates which were favorable to combine with small-molecular free radicals, such as -H, -CH_3 or -OCH_3 to form monophenols. Meanwhile, the breaking of C-O-C and C-C might be enhanced due to the pretreatment of nickel nitrate, yielding more monophenols. In "Ni-unwashed", the contents of phenol, guaiacol, and syringol decreased apparently and it could be inferred that the breakage of C_1-C_α in lignin structure was inhibited in pyrolysis. Whereas the contents of 4-ethylphenol and 4-ethylguaiacol decreased obviously balanced by an increase of 4-vinylphenol and 4-vinylguaiacol. It was surmised that the dehydration of C_α-OH to form C_α=C_β in the side chain was enhanced in pyrolysis, indicating that the existence of nickel influenced the pyrolysis mechanism of lignin to selectively produce vinyl-monophenols. The yields of compounds in G and S types decreased at the same time, whereas the yields of compounds in H type showed little difference. It was speculated that the depolymerization of compounds in G and S types from lignin structure were inhibited.

Many reaction pathways for the formation of these products have been proposed, such as those by Zhang et al. [9] and Wang et al. [31]. According to those propositions and the results of this work, the possible pathways of lignin pyrolysis were proposed as shown in Figure 4. In pyrolysis, different types of free radicals were formed such as -H, -CH_3, -OCH_3 and phenolic radicals. When OL was pretreated with pure water, mainly the cleavage of C-O-C (α-O-4 and β-O-4) and C-C (C_1-C_α) occurred. Except for monophenols, phenolic radicals were bonded together to form large-molecular oligomers as well. When OL was pretreated with $Ni(NO_3)_2$ and washed, the nickel species bonded with lignin which promoted the intermediates to combine with -H, -CH_3, -OCH_3 to yield more monophenols. According to Terakado et al. [39], the thermal degradation of $Ni(NO_3)_2 \cdot 6H_2O$ started with dehydration and then $Ni(NO_3)_2$ was converted into NiO at the temperature between 210–310 °C. While lignin of "Ni-unwashed" pyrolyzed at 500 °C, it was indicated that Ni^{2+} could be reduced to Ni^0 by reductive species (carbon, H_2, CO, and CH_4) derived from pyrolysis. In the presence of Ni^0, the breakage of C_1-C_α was inhibited and the dehydration of C_α-OH was enhanced, respectively in pyrolysis of "Ni-unwashed". Meanwhile, it was also possible that the depolymerization of lignin was inhibited, especially the degradation of compounds in G and S types.
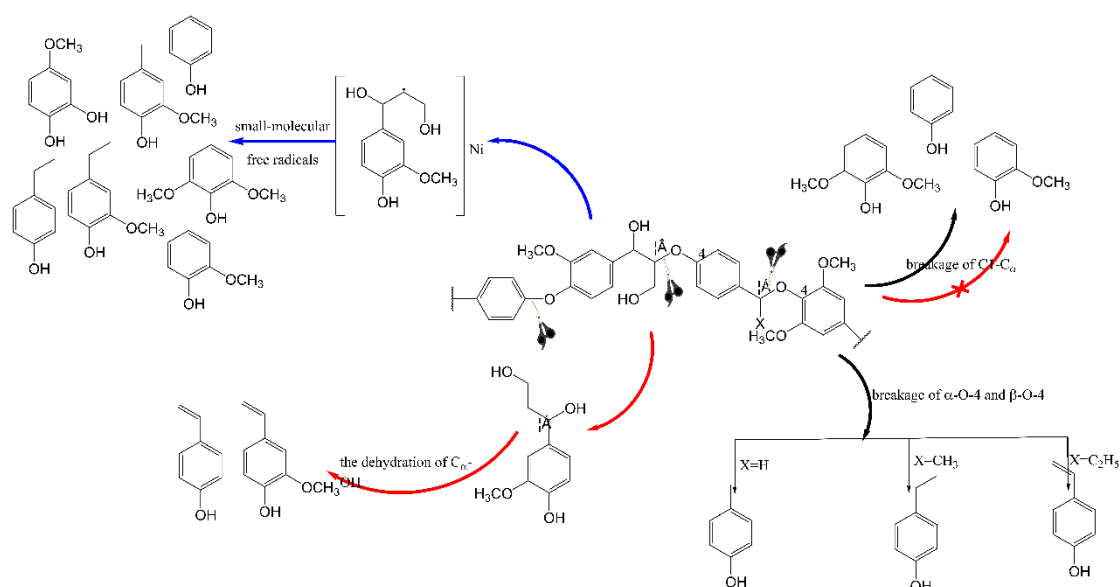
Figure 4. Proposed pathways of lignin pyrolysis (The black arrows represent pathways in "Water"; The blue arrows represent pathway in "Ni-washed"; The red arrows represent pathways in "Ni-unwashed").

3.3.2. Phenolic Oligomers in Bio-Oil

About 70–80 *wt.%* substances in bio-oil obtained from lignin pyrolysis still remained unknown; therefore, ESI-MS, GPC and 2D HSQC NMR were used to comprehensively describe the characteristics of bio-oil.

GPC was selected to probe the molecular weight distribution of products in bio-oil. Because of the limit in molecular weight range of polystyrene standards, only the data above 256 Da were considered convincing. According to the data detected, Mn of the compounds obtained in bio-oil were divided into four parts: 256–500 Da, 500–801 Da, 801–1001 Da and >1001 Da. The results of GPC were shown in Figure 5. Among the three groups, Mn between 256–500 Da was the major species, accounting for the largest proportion. Compared with "Water", Mn between 256–500 Da in "Ni-washed" and "Ni-unwashed" decreased slightly from 85.8 *wt.%* to 82.5 *wt.%* and 78.0 *wt.%*, respectively, while Mn = 500–801 Da, 801–1001 Da and >1001 Da all increased. This revealed that the pretreatment of $Ni(NO_3)_2$ or catalytic performance caused by residual nickel species both inhibited the depolymerization of lignin to small-molecular oligomers. In "Ni-unwashed", the combined effect of pretreatment and catalytic performance made depolymerization of lignin more difficult.
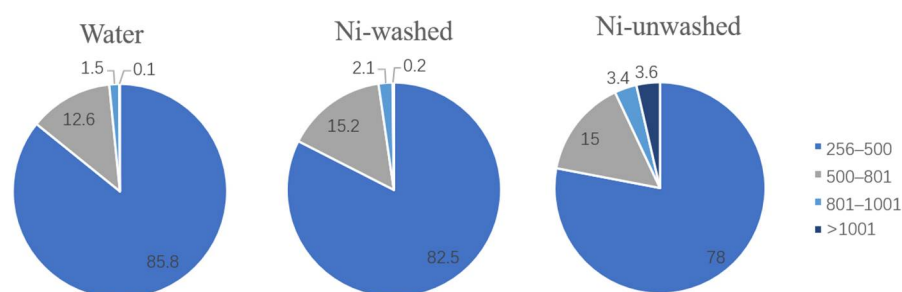
Figure 5. The molecular weight distribution of compounds in bio-oil.

To further analyze and identify the presence of part of monomers and oligomers, ESI-MS in the range of $m/z = 200,500$ was analyzed. According to the molecular weight distribution from GPC, m/z of the substances from ESI-MS and signals of intramolecular C-H bond from 2D HSQC NMR, the possible compounds existed in the bio-oil were listed

in Figure 6. These compounds listed could be found in the work of Fu et al. [40], where characteristic monomers and oligomers were detected and affirmed by ESI-MS and MS^n.
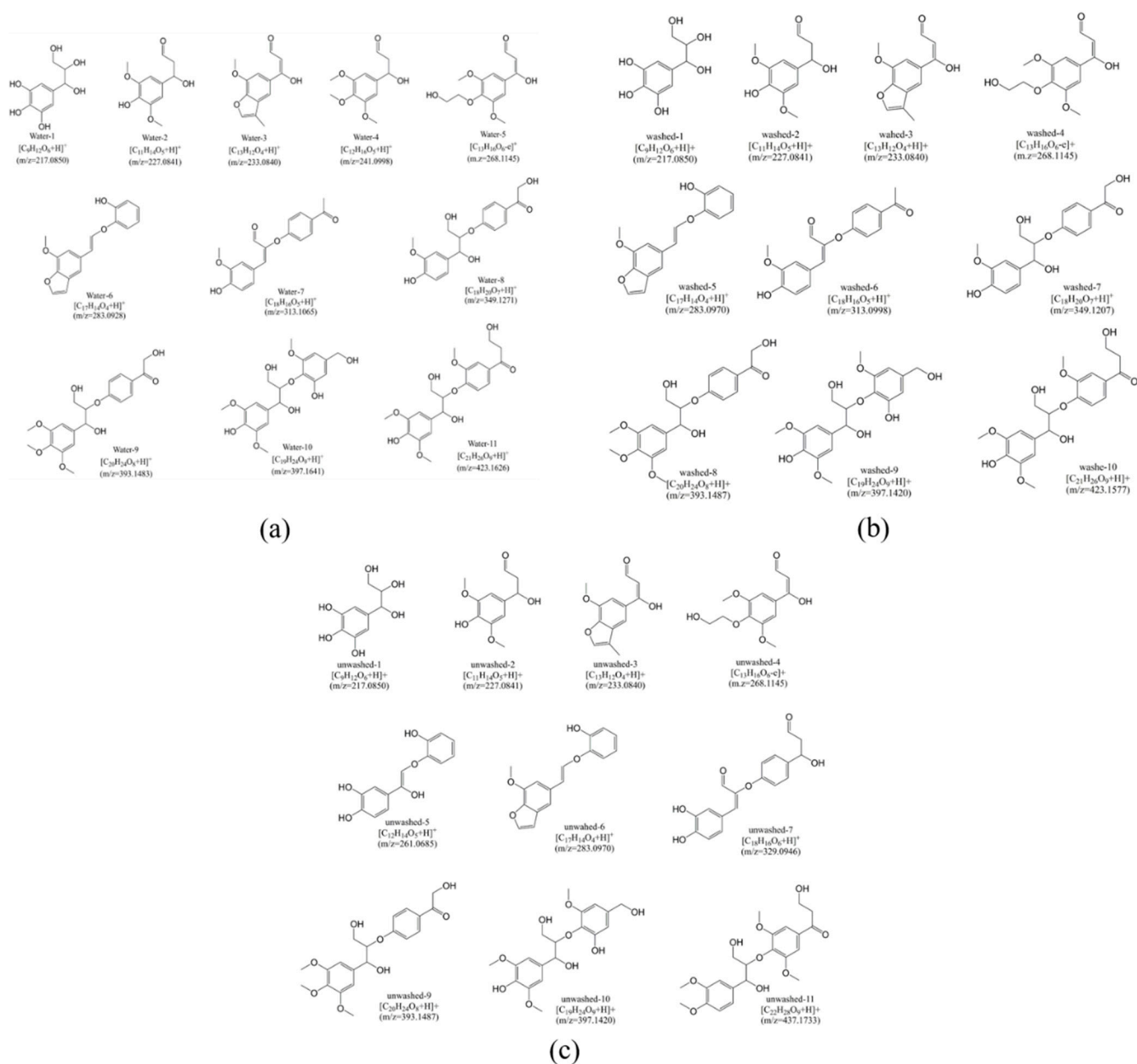
Figure 6. The structure of lignin-derived monomers and oligomers. (**a**) detected in "Water"; (**b**) detected in "Ni-washed"; (**c**) detected in "Ni-unwashed".

Among these substances, 5 monophenols were detected in "Water" while there were 3 in "Ni-washed" and 4 in "Ni-unwashed", respectively. However, the monophenol of m/z = 241 was not found in "Ni-washed" and "Ni-unwashed", which indicated that the pretreatment of $Ni(NO_3)_2$ influenced the derivation of this species, and the possible derivation pathway of this monophenol was shown in Figure 7. Meanwhile, the catalytic performance of nickel species that remained in "Ni-unwashed" apparently changed the pyrolysis mechanism of lignin in comparison with "Water". While the new species of m/z = 261, 329, and 437 were only detected in "Ni-unwashed" and the species of m/z = 313, 349 and 423 of "Water" disappeared in "Ni-unwashed". As speculated, the formation of oligomers contained G units (m/z = 313 and 349) were inhibited and a decrease of monophenols in G type was shown in the results of GC-FID. In addition, the catalytic performance of

nickel that remained in "Ni-unwashed" showed a promotion of reformation of side chain in G units to two -OH (m/z = 261 and 329) or two -OCH$_3$ (m/z = 437). In summary, the degradation of G units in lignin structure was inhibited with the catalytic performance of nickel species and it also could be due to steric effects of -OCH$_3$ at C$_2$ or C$_6$ position. These propositions were consistent with the results from GPC and GC-FID.
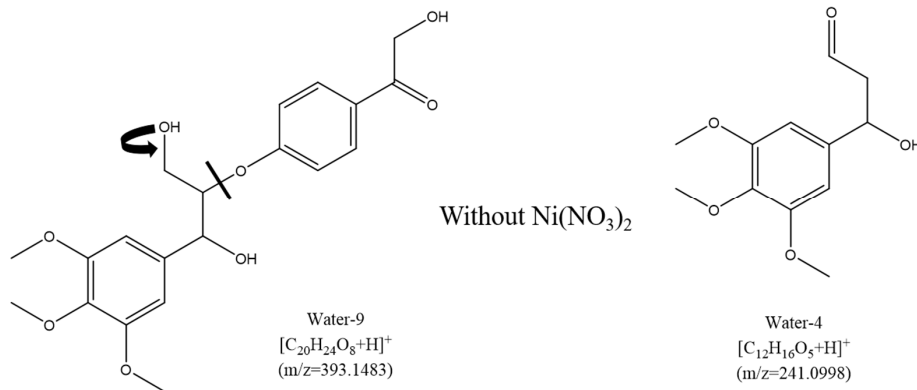
Figure 7. Proposed pathway for the formation of species of m/z = 241 in "Water".

Characteristics of C-H bond of compounds in bio-oil were analyzed and shown in Figure 8. The 2D HSQC NMR spectra were divided into two regions, aromatic (δC/δH = 95−120/5.5−8.0 ppm) and aliphatic side-chain (δC/δH = 50−95/3.0−5.5 ppm). According to literature [29,41,42], the species of primary units were all found in the three groups, which were C−H in methoxy at δC/δH = 56.4/3.71 ppm, C$_\gamma$−H$_\gamma$ in β-O-4 substructures at δC/δH = 61.0/3.40 ppm, various C$_\gamma$−H$_\gamma$ in side chain at δC/δH = 63.4/3.45 ppm, C$_2$−H$_2$ and C$_5$−H$_5$ in guaiacyl units at δC/δH = 110.9/6.96 and 115.5/6.78 ppm, C$_{2,6}$−H$_{2,6}$ in syringyl units and p-hydroxyphenyl units at δC/δH = 104.6/6.79 and 127.6/7.16 ppm. The signals of C-H bond of compounds in bio-oil obtained from 2D HSQC NMR were consistent with the structures in Figure 6 derived from the results of ESI-MS and GPC.
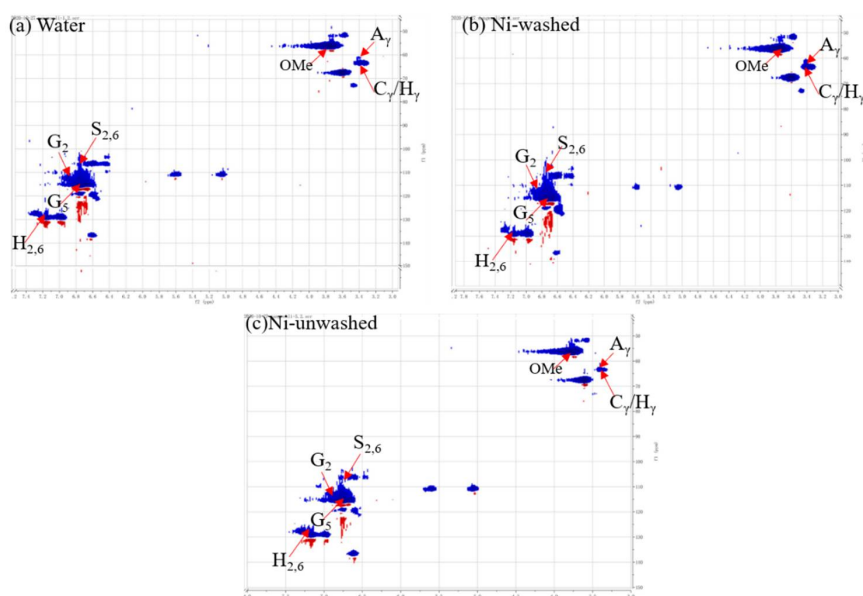
Figure 8. 2D HSQC NMR spectra of bio-oil obtained from lignin pyrolysis.

3.4. The Characteristics of Gaseous Products

$$CH_4 + CO_2 \rightarrow CO + H_2 \tag{8}$$

$$CO + H_2O \rightarrow CO_2 + H_2 \tag{9}$$
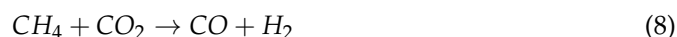
The gas products obtained via pyrolysis were analyzed by GC-TCD as listed in Table 5. Gaseous products mainly included reductive gases (H_2, CO, CH_4) and CO_2. In the "Ni-washed", the yields of H_2 and CO increased apparently balanced with the decrease of CH_4 and CO_2, and it was suggested that carbon dioxide reforming of methane [43] was triggered with the effect of nickel species tightly bonded with the lignin structure as shown in Equation (8). In "Ni-unwashed", the yields of H_2 and CO_2 increased dramatically at a sacrifice of CO and CH_4. Nickel species remained in "Ni-unwashed" were mainly mixed mechanically in sample and acted as in-situ catalyst which would induce water-gas shift (WGS) shown in Equation (9). It was surmised that water-gas shift reaction behaved strongly while carbon dioxide reforming of methane happened at the same time. Overall, the nickel species derived from "Ni-washed" and "Ni-unwashed" promoted different gas reaction, and further exploration of char contained nickel species would be done.

Table 5. The percentage of each gas in gas products (%).

	H$_2$	CO	CH$_4$	CO$_2$
Water	2.0	31.1	29.3	37.6
Ni-washed	7.6	48.3	14.7	29.4
Ni-unwashed	17.1	8.5	15.3	59.1

The results in Table 5 were the average of two tests.

4. Conclusions

In summary, the pretreatment of Ni(NO$_3$)$_2$ in "Ni-washed" and "Ni-unwashed" significantly influenced the pyrolysis behavior of organsolv lignin and changed the pyrolysis mechanism. In "Ni-washed", the yield of monomers apparently increased from 23.3 to 30.2 *wt.%*, although the distribution of char, gas, and bio-oil products showed no difference. Small-molecular oligomers (Mn = 256–500 Da) decreased while the species in Mn > 500 Da increased, and it was indicated that the pretreatment by Ni(NO$_3$)$_2$ could inhibit the depolymerization of lignin to small-molecular oligomers. Furthermore, carbon dioxide reforming of methane reaction was induced in pyrolysis of "Ni-washed" yielding more CO and H_2. In "Ni-unwashed", the yields of char and gas increased at a sacrifice of the yield of bio-oil, which suggested that the depolymerization of lignin was inhibited but the cleavage of the side chain in lignin structure was promoted in pyrolysis. Meanwhile, the yields of 4-vinylphenols (from 2.7 to 4.4 *wt.%*) and 4-vinylguaiacol (from 1.3 to 2.1 *wt.%*) increased obviously, and it was suggested that cracking of C_β-C_γ and the dehydration of C_α-OH were promoted in pyrolysis to selectively form vinyl-monophenols. HHV of bio-oil derived from "Ni-unwashed" slightly increased from 27.94 mJ/kg to 28.46 mJ/kg. Furthermore, new species that were m/z = 261, 329, and 437 were found in "Ni-unwashed". Finally, water-gas shift (WGS) reaction was promoted, yielding an amount of H_2 (17.1 *wt.%*).

Author Contributions: Conceptualization, W.W. and C.H.; methodology, C.H., Y.L., Y.W. and L.L.; software, Y.L., Y.W.; validation, W.W.; formal analysis, W.W.; investigation, W.W.; resources, W.W.; data curation, W.W.; writing—original draft preparation, W.W.; writing—review and editing, C.H.; visualization, W.W.; supervision, C.H.; project administration, C.H.; funding acquisition, C.H. All authors have read and agreed to the published version of the manuscript.

Conflicts of Interest: The authors declare no conflict of interest.

References

1. Somerville, C.; Youngs, H. Feedstocks for Lignocellulosic Biofuels. *Science* **2010**, *329*, 790–792. [CrossRef] [PubMed]
2. Liu, W.J.; Li, W.W. Fates of Chemical Elements in Biomass during Its Pyrolysis. *Chem. Rev.* **2017**, *117*, 6367–6398. [CrossRef]
3. Sun, Z.; Bottari, G. Complete lignocellulose conversion with integrated catalyst recycling yielding valuable aromatics and fuels. *Nat. Catal.* **2018**, *1*, 82–92. [CrossRef]
4. Lynd, L.R.; Liang, X. Cellulosic ethanol: Status and innovation. *Curr. Opin. Biotechnol.* **2017**, *45*, 202–211. [CrossRef] [PubMed]
5. Ha, J.-M.; Hwang, K.-R. Recent progress in the thermal and catalytic conversion of lignin. *Renew. Sustain. Energy Rev.* **2019**, *111*, 422–441. [CrossRef]
6. Lahive, C.W.; Kamer, P.C.J. An Introduction to Model Compounds of Lignin Linking Motifs; Synthesis and Selection Considerations for Reactivity Studies. *ChemSusChem* **2020**, *13*, 4238–4265. [CrossRef]
7. Jiang, Z.; Hu, C. Selective extraction and conversion of lignin in actual biomass to monophenols: A review. *J. Eng. Chem.* **2016**, *25*, 947–956. [CrossRef]
8. Vispute, T.P.; Zhang, H. Renewable Chemical Commodity Feedstocks from Integrated Catalytic Processing of Pyrolysis Oils. *Science* **2010**, *330*, 1222–1227. [CrossRef]
9. Zhang, X.; Jiang, W. Relationship between the formation of oligomers and monophenols and lignin structure during pyrolysis process. *Fuel* **2020**, *276*, 118048. [CrossRef]
10. Liu, Y.; Wang, Y. Effects of MgCl2 Solution Pretreatment at Room Temperature on the Pyrolytic Behavior of Pubescens and the Properties of Bio-oil Obtained. *Energy Fuels* **2020**, *34*, 12665–12677. [CrossRef]
11. Wang, S.; Li, Z. Influence of inherent hierarchical porous char with alkali and alkaline earth metallic species on lignin pyrolysis. *Bioresour. Technol.* **2018**, *268*, 323–331. [CrossRef] [PubMed]
12. Singh, J.; Suhag, M. Augmented digestion of lignocellulose by steam explosion, acid and alkaline pretreatment methods: A review. *Carbohydr. Polym.* **2015**, *117*, 624–631. [CrossRef]
13. Kristiani, A.; Abimanyu, H. Effect of Pretreatment Process by Using Diluted Acid to Characteristic of oil Palm's Frond. *Energy Procedia* **2013**, *32*, 183–189. [CrossRef]
14. Chiesa, S.; Gnansounou, E. Use of Empty Fruit Bunches from the Oil Palm for bioethanol production: A thorough comparison between dilute acid and dilute alkali pretreatment. *Bioresour. Technol.* **2014**, *159*, 355–364. [CrossRef] [PubMed]
15. Cara, C.; Ruiz, E. Production, purification and characterisation of oligosaccharides from olive tree pruning autohydrolysis. *Ind. Crops Prod.* **2012**, *40*, 225–231. [CrossRef]
16. Tan, H.T.; Lee, K.T. Understanding the impact of ionic liquid pretreatment on biomass and enzymatic hydrolysis. *Chem. Eng. J.* **2012**, *183*, 448–458. [CrossRef]
17. Loow, Y.-L.; Wu, T.Y. Recent Advances in the Application of Inorganic Salt Pretreatment for Transforming Lignocellulosic Biomass into Reducing Sugars. *J. Agric. Food. Chem.* **2015**, *63*, 8349–8363. [CrossRef] [PubMed]
18. Wang, Y.; Lv, X. Room temperature pretreatment of pubescens by AlCl3 aqueous solution. *J. Eng. Chem.* **2019**, *31*, 138–147. [CrossRef]
19. Wu, X.; Huang, C. Use of metal chlorides during waste wheat straw autohydrolysis to overcome the self-buffering effect. *Bioresour. Technol.* **2018**, *268*, 259–265. [CrossRef]
20. Wang, Y.; Liu, Y. Torrefaction at 200 °C of Pubescens Pretreated with AlCl3 Aqueous Solution at Room Temperature. *ACS Omega* **2020**, *5*, 27709–27722. [CrossRef]
21. Zhou, S.; Brown, R.C. The use of calcium hydroxide pretreatment to overcome agglomeration of technical lignin during fast pyrolysis. *Green Chem.* **2015**, *17*, 4748–4759. [CrossRef]
22. Milovanović, J.; Luque, R. Study on the pyrolysis products of two different hardwood lignins in the presence of NiO contained-zeolites. *Biomass Bioenergy* **2017**, *103*, 29–34. [CrossRef]
23. Kim, J.-Y.; Choi, J.W. Effect of molecular size of lignin on the formation of aromatic hydrocarbon during zeolite catalyzed pyrolysis. *Fuel* **2019**, *240*, 92–100. [CrossRef]
24. Guo, D.-L.; Wu, S.-B. Catalytic effects of NaOH and Na2CO3 additives on alkali lignin pyrolysis and gasification. *Appl. Energy* **2012**, *95*, 22–30. [CrossRef]
25. Mullen, C.A.; Boateng, A.A. Catalytic pyrolysis-GC/MS of lignin from several sources. *Fuel Process. Technol.* **2010**, *91*, 1446–1458. [CrossRef]
26. Eibner, S.; Broust, F. Catalytic effect of metal nitrate salts during pyrolysis of impregnated biomass. *J. Anal. Appl. Pyrolysis* **2015**, *113*, 143–152. [CrossRef]
27. Custodis, V.B.F.; Karakoulia, S.A. Catalytic Fast Pyrolysis of Lignin over High-Surface-Area Mesoporous Aluminosilicates: Effect of Porosity and Acidity. *ChemSusChem* **2016**, *9*, 1134–1145. [CrossRef]
28. Zhang, H. Performances of Several Solvents on the Cleavage of Interand. *ChemSusChem* **2018**, *11*, 1494–1504. [CrossRef]
29. Lv, X.; Li, Q. Structure characterization and pyrolysis behavior of organosolv lignin isolated from corncob residue. *J. Anal. Appl. Pyrolysis* **2018**, *136*, 115–124. [CrossRef]
30. Bru, K.; Blin, J. Pyrolysis of metal impregnated biomass: An innovative catalytic way to produce gas fuel. *J. Anal. Appl. Pyrolysis* **2007**, *78*, 291–300. [CrossRef]
31. Wang, L.; Li, J. Investigation of the pyrolysis characteristics of guaiacol lignin using combined Py-GC×GC/TOF-MS and in-situ FTIR. *Fuel* **2019**, *251*, 496–505. [CrossRef]

32. Tan, S.S.Y.; MacFarlane, D.R. Extraction of lignin from lignocellulose at atmospheric pressure using alkylbenzenesulfonate ionic liquid. *Green Chem.* **2009**, *11*, 339–345. [CrossRef]

33. Chen, L.; Wang, X. Study on pyrolysis behaviors of non-woody lignins with TG-FTIR and Py-GC/MS. *J. Anal. Appl. Pyrolysis* **2015**, *113*, 499–507. [CrossRef]

34. Tayier, M.; Zhao, Y. Bamboo biochar-catalytic degradation of lignin under microwave heating. *J. Wood Chem. Technol.* **2020**, *40*, 190–199. [CrossRef]

35. Norouzi, O.; Kheradmand, A. Superior activity of metal oxide biochar composite in hydrogen evolution under artificial solar irradiation: A promising alternative to conventional metal-based photocatalysts. *Int. J. Hydrogen Energy* **2019**, *44*, 28698–28708. [CrossRef]

36. Collard, F.-X.; Blin, J. Influence of impregnated metal on the pyrolysis conversion of biomass constituents. *J. Anal. Appl. Pyrolysis* **2012**, *95*, 213–226. [CrossRef]

37. Collard, F.-X.; Bensakhria, A. Influence of impregnated iron and nickel on the pyrolysis of cellulose. *Biomass Bioenergy* **2015**, *80*, 52–62. [CrossRef]

38. Liu, C.; Hu, J. Thermal conversion of lignin to phenols: Relevance between chemical structure and pyrolysis behaviors. *Fuel* **2016**, *182*, 864–870. [CrossRef]

39. Terakado, O.; Amano, A. Explosive degradation of woody biomass under the presence of metal nitrates. *J. Anal. Appl. Pyrolysis* **2009**, *85*, 231–236. [CrossRef]

40. Fu, X.; Li, Q. Identification and structural characterization of oligomers formed from the pyrolysis of biomass. *J. Anal. Appl. Pyrolysis* **2019**, *144*, 104696.1–104696.10. [CrossRef]

41. del Rio, J.C.; Rencoret, J. Structural characterization of wheat straw lignin as revealed by analytical pyrolysis, 2D-NMR, and reductive cleavage methods. *J. Agric. Food. Chem.* **2012**, *60*, 5922–5935. [CrossRef] [PubMed]

42. Yang, S.; Yuan, T.-Q. Structural Elucidation of Whole Lignin in Cell Walls of Triploid of Populus tomentosa Carr. *ACS Sustain. Chem. Eng.* **2016**, *4*, 1006–1015. [CrossRef]

43. Wang, Y.; Yao, L. Low-Temperature Catalytic CO_2 Dry Reforming of Methane on Ni-Si/ZrO_2 Catalyst. *ACS Catal.* **2018**, *8*, 6495–6506. [CrossRef]